

Topological nonsymmorphic crystalline insulators

Chao-Xing Liu,¹ Rui-Xing Zhang,¹ and Brian K. VanLeeuwen²

¹*Department of Physics, The Pennsylvania State University, University Park, Pennsylvania 16802-6300, USA*

²*Department of Materials Science and Engineering, The Pennsylvania State University, University Park, Pennsylvania 16802, USA*

(Received 24 August 2013; revised manuscript received 29 June 2014; published 11 August 2014)

In this work, we identify a class of topological phases protected by nonsymmorphic crystalline symmetry dubbed “topological nonsymmorphic crystalline insulators.” We construct a concrete tight-binding model for a lattice with nonsymmorphic symmetry and confirm its topological nature by directly calculating topological surface states. Analogous to “Kramers’ pairs” originating from time-reversal symmetry, we introduce “doublet pairs” originating from nonsymmorphic symmetry to define the corresponding Z_2 topological invariant for this phase. Based on projective representation theory, we extend our discussion to other nonsymmorphic symmetry groups that can host this topological phase which will provide guidance for the systematic search for new topological materials.

DOI: [10.1103/PhysRevB.90.085304](https://doi.org/10.1103/PhysRevB.90.085304)

PACS number(s): 73.20.At, 73.43.-f, 02.20.-a

I. INTRODUCTION

The search for new states of matter, especially those with nontrivial topological properties, is one of the main focuses of condensed-matter physics. The recent experimental discovery of time-reversal (TR) invariant topological insulators (TIs) [1–4] has inspired lots of research interest and led to the rapid development of this field. TR invariant TIs possess insulating bulk states and metallic edge/surface states that are protected by TR symmetry due to the double degeneracy guaranteed by Kramers’ theorem [5]. In principle, degeneracies can also come from other types of symmetries, such as crystalline symmetry, etc. Therefore, it is natural to ask if one can find new topological phases (TPs) protected by other symmetries. Several recent theoretical works [6–17] are devoted to TPs protected by crystalline symmetry dubbed topological crystalline insulators (TCIs). Recent experimental observations of surface states in the SnTe family of materials confirm the theoretical prediction of TCIs protected by mirror symmetry [18–20].

Nonsymmorphic symmetry groups possess operations combining a point symmetry operation and a nonprimitive translation operation which cannot be removed by changing the origin [21,22]. It is known that nonsymmorphic symmetries can “stick bands together” and yield extra degeneracies. Most studies of TCIs have focused on point groups or symmorphic space groups and it is still unclear if nonsymmorphic symmetries can yield new TCIs. In this paper, we give an affirmative answer to this question by constructing a concrete example and identifying a class of Z_2 TPs as a direct physical consequence of noncommutativity of symmetry operators in nonsymmorphic groups. Consequently, we name them topological nonsymmorphic crystalline insulators (TNCIs). We construct a new Z_2 topological invariant for this phase which can be evaluated numerically by the Wilson loop approach [23]. Our general discussion of nonsymmorphic space groups will provide guidance to the search for realistic materials with the TNCI phase.

II. TIGHT-BINDING MODEL

We start from a concrete tight-binding model of TNCIs. The aim of this model is to demonstrate that gapless surface states, as well as topological properties, are protected by

nonsymmorphic symmetry, instead of any other symmetry, such as TR symmetry [1–4] or other antiunitary symmetries [24–26]. Therefore, we need to break ALL the antiunitary symmetries in the model explicitly. As shown in Fig. 1(a), our tight-binding model has a layered antiferromagnetic structure stacked along the z direction, where each layer is a square lattice with magnetic moments on each site perpendicular to the xy plane. Magnetic moments in each layer are ordered ferromagnetically. However, the magnetization directions between two adjacent layers are opposite, i.e., the whole system has an antiferromagnetic structure with two atoms in one unit cell, denoted as A and B . The lattice vectors are denoted as $\vec{a}_1 = (a, 0, 0)$, $\vec{a}_2 = (0, b, 0)$, and $\vec{a}_3 = (0, 0, c)$. In a unit cell, the A and B atoms are shifted in opposite directions along the x axis. The position of the A atom is $r_A = (-a_1, 0, 0)$ while that of the B atom is $r_B = (a_1, 0, \frac{c}{2})$ as shown in Fig. 1(a). This configuration has $Pma2$ -type space-group symmetry. Each lattice site contains three orbitals, $|s\rangle$, $|p_x\rangle$, and $|p_y\rangle$. The $|p_x\rangle$ and $|p_y\rangle$ orbitals carry the angular momentum 1 and couple to magnetic moments through Zeeman-type coupling, denoted as M_1 . The explicit form of our Hamiltonian is shown in the Supplemental Material [27] and is written under the basis $|\alpha\eta, \vec{k}\rangle = \frac{1}{\sqrt{N}} \sum_n e^{i\vec{k}\cdot\vec{r}_{n\eta}} \phi_\alpha(\vec{r} - \vec{r}_{n\eta})$ where N is the normalization factor, $\vec{r}_{n\eta} = \vec{R}_n + \vec{r}_\eta$ with the lattice vector \vec{R}_n and the position \vec{r}_η of the atom $\eta = A, B$, and ϕ_α denotes the basis wave function ($\alpha = s, p_x, p_y$).

Our model is similar to that discussed previously by one of the authors [26], where the antiunitary operation combining TR with translation plays an essential role. However, in the present model, the shift of the A and B atoms in opposite directions breaks this antiunitary symmetry. Instead, it turns out that two unitary operators are essential. One is the mirror symmetry along the z direction, denoted as $\hat{m}_z = \{\hat{m}_z | \vec{e}\} : (x, y, z) \rightarrow (x, y, -z)$ where $\vec{e} = (0, 0, 0)$, and the other is the glide symmetry, $\hat{g}_x = \{\hat{m}_x | \vec{\tau}\} : (x, y, z) \rightarrow (-x, y, z + \frac{c}{2})$ with $\vec{\tau} = \frac{\vec{a}_3}{2} = (0, 0, \frac{c}{2})$. When restricted to the xz plane, these two symmetry operations, together with translation in the xz plane, give the two-dimensional (2D) nonsymmorphic space group pmg . Direct calculation gives

$$\hat{m}_z \hat{g}_x = \{C_{2y} | -\vec{\tau}\} \neq \hat{g}_x \hat{m}_z = \{C_{2y} | \vec{\tau}\}, \quad (1)$$

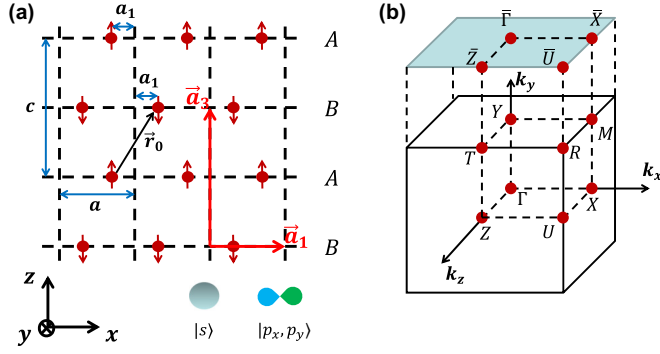


FIG. 1. (Color online) (a) Lattice sites in the xz plane for our tight-binding model. The lattice vectors \vec{a}_1 and \vec{a}_3 are shown in the figure and \vec{a}_2 is perpendicular to this plane (y direction). (b) The bulk Brillouin zone (BZ) and the surface BZ for the xz plane.

where C_{2y} is a twofold rotation around the y axis. The noncommutativity between \hat{g}_x and \hat{m}_z is essential, as discussed below.

Let us first analyze symmetry properties of our tight-binding Hamiltonian. The symmetry operators \hat{m}_z and \hat{g}_x act on the basis $|\alpha\eta, \vec{k}\rangle$ such that $\hat{m}_z|\alpha\eta, \vec{k}\rangle = |\alpha\eta, \hat{m}_z\vec{k}\rangle$ and $\hat{g}_x|\alpha\eta, \vec{k}\rangle = \sum_{\beta} e^{-ik_z c/2} m_{x,\alpha\beta} |\beta\bar{\eta}, \hat{m}_x\vec{k}\rangle$ where $\bar{\eta}$ is the interchange of the A and B indices and the 3×3 matrix $m_x = \text{Diag}[1, -1, 1]$ in the basis $|s\rangle, |p_x\rangle, |p_y\rangle$. For a symmetry operation \hat{U} , the Hamiltonian should satisfy $H(\vec{k}) = U^*(\vec{k})H(\hat{U}\vec{k})U^T(\vec{k})$. The details about how these symmetries constrain the form of Hamiltonian are shown in the Supplemental Material [27] and we focus on the $k_z = \frac{\pi}{c}$ plane here. Since $|\alpha\eta, \vec{k} + \vec{G}\rangle = e^{i\vec{G}\cdot\vec{r}_\eta} |\alpha\eta, \vec{k}\rangle$, the off-diagonal part Hamiltonian $H_{AB}(\vec{k})$ is not periodic, but satisfies the relation $H_{AB}(\vec{k} + \vec{G}) = e^{i\vec{G}\cdot\vec{r}_0} H_{AB}(\vec{k})$ where $\vec{r}_0 = \vec{r}_B - \vec{r}_A$. At $k_z = \pi/c$, one has $H_{AB}(k_x, k_y, \frac{\pi}{c}) = -H_{AB}(k_x, k_y, -\frac{\pi}{c})$. Due to mirror symmetry \hat{m}_z , $H_{AB}(k_x, k_y, \frac{\pi}{c}) = H_{AB}(k_x, k_y, -\frac{\pi}{c})$, so $H_{AB}(k_x, k_y, \frac{\pi}{c}) = 0$. There is no coupling between the A and B layers and the Hamiltonian is block-diagonal in the $k_z = \pi/c$ plane. We will denote the momentum in the $k_z = \pi/c$ plane by $\vec{k} = (k_x, k_y, \frac{\pi}{c})$ below. If $|\phi_{A,\vec{k}}\rangle$ is an eigenstate of $H_A(\vec{k})$ with eigenenergy $E_{A,\vec{k}}$, then $|\phi_{B,\hat{m}_x\vec{k}}\rangle = \hat{g}_x|\phi_{A,\vec{k}}\rangle$ is an eigenstate of $H_B(\hat{m}_x\vec{k})$ with the same eigenenergy [i.e., $H_B(\hat{m}_x\vec{k})|\phi_{B,\hat{m}_x\vec{k}}\rangle = E_{A,\vec{k}}|\phi_{B,\hat{m}_x\vec{k}}\rangle$]. Therefore, $|\phi_{A,\vec{k}}\rangle$ is degenerate with $|\phi_{B,\hat{m}_x\vec{k}}\rangle$ at the $k_z = \frac{\pi}{c}$ plane. For two lines $\vec{k} = (0, k_y, \frac{\pi}{c})$ and $\vec{k} = (\frac{\pi}{a}, k_y, \frac{\pi}{c})$ that satisfy $\hat{m}_x\vec{k} = \vec{k}$, all the electronic states are doubly degenerate.

To confirm the existence of TPs in our model, we perform an electronic structure calculation for a slab configuration with finite lattice sites along the y direction. Since the surface of the slab is normal to the y direction, the symmetries \hat{m}_z and \hat{g}_x are preserved. We find that when the coupling M_1 between magnetization and p orbitals is small, there are no surface states [Fig. 2(a)]. But when M_1 exceeds a critical value, the Dirac type of surface states appear around \bar{Z} , as shown in Fig. 2(b). The degeneracy at the \bar{Z} Dirac point is due to two unitary symmetry operators \hat{m}_z and \hat{g}_x , as shown above. It is impossible to remove the surface states in Fig. 2(b) without closing the bulk band gap if the pmg symmetry is preserved

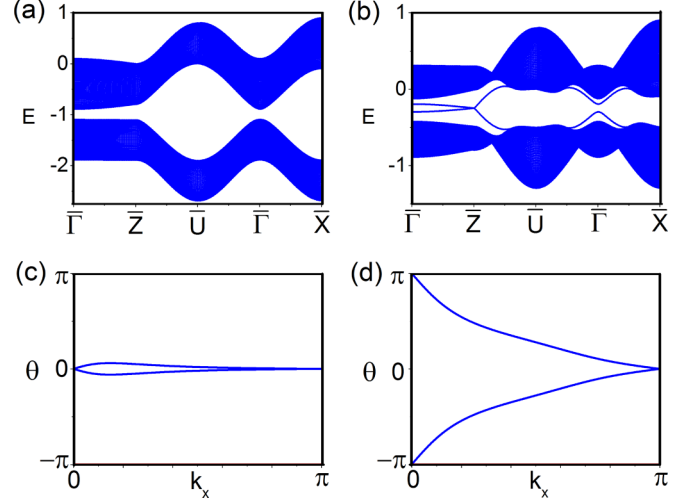


FIG. 2. (Color online) Energy dispersion of a slab configuration for our tight-binding model with the parameter (a) $M_1 = 3.1$ and (b) $M_1 = 4.5$. The corresponding evolution of Wannier function centers in a 3D bulk system is shown as a function of k_x for (c) $M_1 = 3.1$ and (d) $M_1 = 4.5$. The surface states in (b) and the winding number of Wannier function centers in (d) indicate that the system is in the TNCI phase for $M_1 = 4.5$.

in the xz plane. We therefore expect that a topological phase protected by the pmg symmetry exists in this system.

III. Z_2 TOPOLOGICAL INVARIANT

To confirm the topological nature of two-dimensional (2D) surface states, it is necessary to construct a topological invariant for the three-dimensional (3D) bulk system. The Z_2 topological invariant in TR invariant TIs is defined by the Pfaffian of the antisymmetric matrix of the TR operator in the occupied band subspace [5,28]. However, only unitary symmetry operators are involved in our model, so there is no antiunitary operator to replace the TR operator to define topological invariants. Nevertheless, we can still separate all the occupied states into two sets and introduce the concept of “partial polarization” for each set [28]. The Z_2 topological invariant can be defined by tracking the evolution of partial polarizations of doublets.

We start by identifying two sets of degenerate eigenstates for a generic system with pmg symmetry. Since the Hamiltonian has \hat{m}_z symmetry, one can find the common eigenstates of $H(\vec{k})$ and \hat{m}_z at the $k_z = 0$ and $k_z = \pi/c$ plane. We consider the $k_z = \pi/c$ plane and take one common eigenstate $|\phi_{\vec{k}}^I\rangle$ given by $H(\vec{k})|\phi_{\vec{k}}^I\rangle = E_{I,\vec{k}}|\phi_{\vec{k}}^I\rangle$ and $\hat{m}_z|\phi_{\vec{k}}^I\rangle = m_z|\phi_{\vec{k}}^I\rangle$. One can define a state $|\phi_{\hat{m}_x\vec{k}}^{II}\rangle = e^{i\chi_{\vec{k}}} \hat{g}_x|\phi_{\vec{k}}^I\rangle$, which is an eigenstate of $H(\hat{m}_x\vec{k})$ with the same eigenenergy $E_{I,\vec{k}}$, but acquires a phase shift $\chi_{\vec{k}}$. Moreover, according to (1), direct calculation shows $\hat{m}_z \hat{g}_x |\phi_{\vec{k}}^\alpha\rangle = iC_{2y} |\phi_{\vec{k}}^\alpha\rangle$ and $\hat{g}_x \hat{m}_z |\phi_{\vec{k}}^\alpha\rangle = -iC_{2y} |\phi_{\vec{k}}^\alpha\rangle$ ($\alpha = I, II$), so the representation matrices of \hat{m}_z and \hat{g}_x on the basis $|\phi_{\vec{k}}^\alpha\rangle$ anticommute with each other at the $k_z = \pi/c$ plane, which indicates that the mirror parity of $|\phi_{\hat{m}_x\vec{k}}^{II}\rangle$ is $-m_z$, opposite to that of $|\phi_{\vec{k}}^I\rangle$. Therefore, one finds two distinct sets of eigenstates, dubbed “doublet pairs” below.

With doublet pairs, we can define the partial polarization as $P_\alpha(k_x) = \frac{1}{2\pi} \oint dk_y \langle \phi_{\vec{k}}^\alpha | i \partial_{k_y} | \phi_{\vec{k}}^\alpha \rangle$ ($\alpha = I, II$). The partial polarizations of doublet pairs can be related to each other by

$$P_{II}(-k_x) = P_I(k_x) - \frac{1}{2\pi} (\chi_{\pi/a} - \chi_{-\pi/a}). \quad (2)$$

Due to the single-valuedness of $|\phi_{\vec{k}}^\alpha\rangle$, the phase $\chi_{\vec{k}}$ can only differ by 2π times an integer when k_x is changed by $2\pi/a$. Thus, Eq. (2) leads to two conclusions: (1) P_{II} at $k_x \in [-\pi/a, 0]$ is determined by P_I at $k_x \in [0, \pi/a]$; (2) at $k_x = 0$ and π/a , P_I is equivalent to P_{II} up to an integer.

The constraint on the partial polarization from Eq. (2) indicates the possibility of defining a Z_2 topological invariant. Based on the method introduced by Yu *et al.* [23], one can obtain the Wannier function centers θ of the occupied bands by calculating the eigenvalues of the non-Abelian Berry connection along the ‘‘Wilson loop.’’ The polarization is related to the sum of Wannier function centers over occupied bands by $P = \frac{1}{2\pi} \sum_{\text{occupied}} \theta$. The Wannier function centers of doublet pairs θ as a function of k_x are shown in Figs. 2(c) and 2(d). One can clearly see the different evolutions of Wannier function centers between topologically trivial and nontrivial phases. Wannier function centers are periodic and only well defined by any integer times 2π . Thus, one can regard the regime $[-\pi, \pi)$ as a ring and consider the evolution of Wannier function centers on this ring. Similar to the case of TR invariant TIs [23], the total winding number of the Wannier function centers of all doublet pairs on this ring defines a Z_2 topological invariant. The pmg symmetry in the xz plane guarantees that the Wannier function centers of doublet pairs must be degenerate at $k_x = 0$ and $k_x = \pi/a$. If the Wannier function centers of all doublet pairs enclose the ring an odd number of times, it is topologically nontrivial. Otherwise, it is topologically trivial. Alternatively, one can define ‘‘doublet polarization’’ $P_d = P_I - P_{II}$, analogous to ‘‘time-reversal polarization’’ as introduced by Fu and Kane [28], and the Z_2 topological invariant can then be defined by the difference $\Delta = P_d(\pi) - P_d(0) \bmod 2$.

IV. OTHER NONSYMMORPHIC GROUPS

We will generalize our discussion to other nonsymmorphic symmetry groups. From the above model, we can see that the degeneracies guaranteed by nonsymmorphic symmetry play an essential role in protecting surface states. However, the symmetry groups of different surfaces are different and not all the 2D surfaces can possess nonsymmorphic symmetry even for a crystal with 3D nonsymmorphic space-group symmetry. Therefore, our strategy is to directly consider a semi-infinite crystal with one specific surface, as shown in Fig. 3(a), of which the symmetry group can be described by a 2D space group. We consider an insulating material in this semi-infinite configuration and assume that the states are doubly degenerate at two high-symmetry momenta (HSM) K_1 and K_2 in the surface Brillouin zone (BZ). As shown in Fig. 3(b), if surface states switch their degenerate partners between K_1 and K_2 , such surface states cannot be adiabatically connected to any trivial state in a 2D system with the same symmetry group. Due to the boundary-bulk correspondence, we expect that TPs

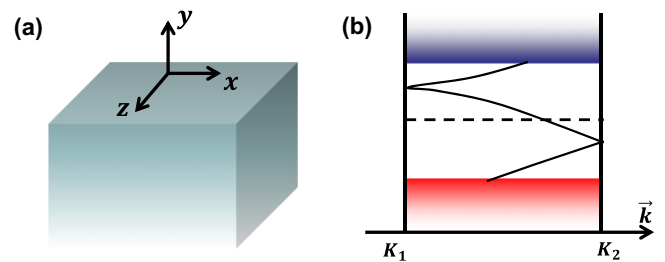


FIG. 3. (Color online) (a) Schematic plot of a semi-infinite crystal with one surface. (b) Energy dispersion of nontrivial surface states. Here \vec{K}_1 and \vec{K}_2 are two HSM.

exist in the corresponding 3D bulk systems. In two dimensions, there are only 17 space groups, so a systematic study of TCIs is possible. We focus on nonsymmorphic symmetry groups here.

The above analysis has shown the importance of symmetry induced degeneracy. The degeneracies of electronic states in a system correspond to the dimensions of the irreducible representations (IRs) of its symmetry group [21,22], i.e., the group representation of the symmetry group on a set of n degenerate eigenstates is a n -dimensional IR. In a space group, symmetry operations at a fixed momentum form a subgroup of the whole group, known as a wave-vector group. Consequently, the degeneracies of electronic states at a certain momentum are determined by the dimensions of the IRs of the wave-vector group. For the 2D nonsymmorphic space groups considered here, it turns out that only four HSM, $\bar{\Gamma}$, \bar{X} , \bar{Z} , and \bar{U} , in Fig. 1(b) possess wave-vector groups of pmg symmetry.

The uniqueness of a nonsymmorphic group lies in the structure of its representations [22]. Although the factor group of a nonsymmorphic space group with respect to its translational subgroup is isomorphic to a point group, its representation is not identical to the conventional representation of a point group. For an element $\{S|\vec{R}\}$ in a space group, the corresponding representation matrix at a momentum \vec{k} takes the form $D_{\vec{k}}(\{S|\vec{R}\}) = e^{i\vec{k}\cdot\vec{R}} D(S)$. The matrix $D(S)$, that only depends on the point-group operation (i.e., the linear part of the space-group motion), satisfies the multiplication rule $D(S_1)D(S_2) = \omega(S_1, S_2)D(S_1 S_2)$ for two symmetry operators $\{S_1|\vec{R}_1\}$ and $\{S_2|\vec{R}_2\}$ in the wave-vector group, where ω is a phase given by $\omega(S_1, S_2) = e^{i(\vec{k}-S_1^{-1}\vec{k})\cdot\vec{R}_2}$ and it defines a so-called factor system [22]. The additional phase coefficient appearing in the multiplication rules indicates that projective representations of a point group, instead of conventional representations, are required for a nonsymmorphic symmetry group. The projective representations are usually classified into different classes by their factor systems. To determine the class for a wave-vector group, one can consider the parameter $\alpha = \omega(S_1, S_2)/\omega(S_2, S_1)$, where S_1 commutes with S_2 . For a crystalline symmetry group, α can only take values of ± 1 . If $\alpha = 1$, the projective representation belongs to a class identical to the conventional representation, denoted as K_0 . If $\alpha = -1$, the projective representation belongs to a nontrivial class, usually denoted as K_1 .

We may consider our example of pmg group. The corresponding factor group is isomorphic to the D_2 group. The K_0 class is the same as the conventional representation,

which only contains 1D IRs, while the K_1 class of D_2 group has one 2D IRs, which indicates the double degeneracy at HSM. In the surface BZ [Fig. 1(b)], only four momenta $\vec{K} = \vec{\Gamma}, \vec{X}, \vec{Z}, \vec{U}$ contain all the symmetry operations in pmg group. For the operators \hat{m}_z and $\hat{g}_x = \{\hat{m}_x | \vec{\tau}\}$, we have $\alpha = \omega(\hat{m}_z, \hat{m}_x) / \omega(\hat{m}_x, \hat{m}_z) = e^{i\vec{\tau} \cdot (\hat{m}_x^{-1} \vec{K} - \hat{m}_z^{-1} \vec{K})}$. Direct calculation shows $\alpha = 1$ for $\vec{K} = \vec{\Gamma}, \vec{X}$ and $\alpha = -1$ for $\vec{K} = \vec{Z}, \vec{U}$. Therefore, all the states at \vec{Z} and \vec{U} must be doubly degenerate, consistent with the analysis of our concrete tight-binding model.

The analysis based on projective representations can be applied to surfaces with other 2D nonsymmorphic groups, namely pg , pgg , and $p4g$. The surface BZs of these groups are the same as that of the pmg group. Thus, we can use the same notation, as shown in Fig. 1(b), for the BZ of these groups. The classes of the projective representations for HSM $\vec{\Gamma}, \vec{X}, \vec{Z}, \vec{U}$ are summarized in the tables in the Supplemental Material for different nonsymmorphic groups [27]. One finds no Z_2 TPs in pg since all HSM belong to the K_0 class. For both pgg and $p4g$, \vec{X} and \vec{Z} belong to the K_1 class, so topological surface states can exist between \vec{X} and \vec{Z} . For $p4g$, $\vec{\Gamma}$ and \vec{U} belong to the K_0 class of the D_4 group, which contains four 1D IRs and one 2D IR. Therefore, both doublets and singlets exist at these two momenta, similar to the case of $p4m$ [29]. The complete study of TPs in $p4g$ will be given elsewhere. The generalization to spinful fermions is straightforward, as shown in the Supplemental Material. One just needs to take into account the additional phase factor induced by spin.

V. DISCUSSION AND CONCLUSION

The key idea to realize TIs is to find a material with inverted band structure. From the model presented here, one can see that a similar idea can also be applied to the search for realistic materials of TNCIs. The band inversion in our model is induced by the coupling M_1 to magnetization, a mechanism which is similar to that in the quantum anomalous Hall effect, which has been experimentally realized [30]. However, we would like to emphasize that band inversion in principle can also be induced by other mechanisms, such as spin-orbit coupling, strain, etc. For TR invariant TIs, one requires TR symmetry. In contrast, for TNCIs, one needs to look for semiconducting materials that possess surfaces with 2D symmetry groups pmg , pgg , and $p4g$. This is the main motivation for the group theory classification above. It is known that 157 of the 230 space groups are nonsymmorphic and the surfaces with the required symmetry exist in 58 of them [27]. The possible 3D space groups are listed in Table III in the Supplemental Material [27] and a systematic search for TNCIs can be carried out based on this table. In one word, one can search for TNCIs in a system with inverted band structure and with appropriate symmetry groups.

We conclude our discussion with three comments. First, in the TCI model proposed by Fu [6], the existence of singlets weakens the stability of surface states. For nonsymmorphic groups, only doublets can exist at certain HSM and we expect that topological surface states of TNCIs are more robust. Second, our discussion has shown that TNCIs exist in both the single and double group cases. Therefore, unlike TR invariant TIs, this TP is not limited to fermionic systems, but can also

occur in bosonic systems such as photonic crystals [31–33]. Third, we would like to emphasize the difference between our work and previous works [24,26,34,35]. Unlike TPs discussed in Refs. [24,26], which require antiunitary symmetry, TNCIs only require unitary symmetry operators. TNCIs here are also different from “topological orders” studied in Refs. [34,35]. In fact, TNCIs belong to the trivial class using the criterion in Ref. [35], and they represent a new class of “symmetry protected topological orders” [36].

ACKNOWLEDGMENTS

We would like to thank X. Dai, X. Y. Dong, L. Fu, V. Gopalan, X. L. Qi, and Y. H. Wu for useful discussions. We especially acknowledge Y. H. Wu’s careful reading of the manuscript. C.X.L. was supported by startup funds from PSU. B.K.V. was supported by Penn State MRSEC DMR-0820404, and partially by DMR-1210588.

APPENDIX A: TIGHT-BINDING MODEL OF TOPOLOGICAL NONSYMMORPHIC CRYSTALLINE INSULATORS

The tight-binding Hamiltonian of our model is given by

$$H = H_A + H_B + H_{AB}, \quad (A1)$$

$$H_\eta = \sum_{\langle \vec{n}\vec{m} \rangle_{in}, \alpha\beta} t_{\vec{n}\vec{m}}^{\alpha\beta} c_{\alpha\vec{n}\eta}^\dagger c_{\beta\vec{m}\eta} + \sum_{\vec{n}, \alpha} \epsilon_\alpha c_{\alpha\vec{n}\eta}^\dagger c_{\alpha\vec{n}\eta} + \sum_{\vec{n}} \delta_\eta M_1 (-i c_{\vec{n}p_x\eta}^\dagger c_{\vec{n}p_y\eta} + \text{H.c.}), \quad (A2)$$

$$H_{AB} = \sum_{\langle \vec{n}\vec{m} \rangle_{AB}, \alpha\beta} (r_{\vec{n}\vec{m}}^{\alpha\beta} c_{\alpha\vec{n}A}^\dagger c_{\beta\vec{m}B} + \text{H.c.}), \quad (A3)$$

where $\eta = A, B$ is for A, B layers, $\delta_{\eta=A(B)} = +(-)$, $\vec{n} = (n_x, n_y, n_z)$, $\vec{m} = (m_x, m_y, m_z)$ denote lattice sites, and $\alpha, \beta = s, p_x, p_y$ denote orbitals. The term H_A (H_B) comes from hopping terms within the layer consisting of only A (B) atoms while H_{AB} is due to hopping between A and B layers. $\langle \vec{n}\vec{m} \rangle_{in}$ represents nearest neighbors in the xy plane with hopping parameters $t_{\vec{n}\vec{m}}^{\alpha\beta}$ while $\langle \vec{n}\vec{m} \rangle_{AB}$ represents nearest neighbors that reside in two adjacent A and B layers with the parameters $r_{\vec{n}\vec{m}}^{\alpha\beta}$. We take into account the σ bond for the s orbitals, the σ and π bonds for the p orbitals, and the σ bonds between the s and p orbitals. The intralayer hopping parameters are given by the matrices

$$t_{\vec{n}, \vec{n}+\hat{e}_x} = \begin{pmatrix} u_{s\sigma} & u_{sp\sigma} & 0 \\ -u_{sp\sigma} & u_{p\sigma} & 0 \\ 0 & 0 & u_{p\pi} \end{pmatrix}, \quad (A4)$$

$$t_{\vec{n}, \vec{n}+\hat{e}_y} = \begin{pmatrix} u_{s\sigma} & 0 & u_{sp\sigma} \\ 0 & u_{p\pi} & 0 \\ -u_{sp\sigma} & 0 & u_{p\sigma} \end{pmatrix},$$

in the basis $|s\rangle$, $|p_x\rangle$, and $|p_y\rangle$, where \hat{e}_x and \hat{e}_y denote unit vectors to the nearest-neighbor site along the x and y directions, respectively. For the hopping between two layers, since $\vec{r}_0 = \vec{r}_B - \vec{r}_A$ is not along the z direction, we need to decompose the p orbitals into components along the \vec{r}_0 axis

and perpendicular to \vec{r}_0 . Consequently, we obtain

$$r_{\vec{n}, \vec{n}+\vec{r}_0} = \begin{pmatrix} v_{s\sigma} & v_{sp\sigma}\lambda_1 & 0 \\ -v_{sp\sigma}\lambda_1 & v_{p\sigma}\lambda_1^2 + v_{p\sigma}(1-\lambda_1^2) & 0 \\ 0 & 0 & v_{p\pi} \end{pmatrix}, \quad (\text{A5})$$

where $\lambda_1 = \frac{2a_1}{|\vec{r}_0|}$ is the cosine of the angle between \vec{r}_0 and the x axis. The M_1 term is the Zeeman type of coupling between the p orbitals and the magnetic moments. In momentum space, the Hamiltonian is given by

$$H_\eta = \sum_k \Psi_\eta^\dagger \begin{pmatrix} E_s(\vec{k}) & -2iu_{sp\sigma} \sin(k_x a) & -2iu_{sp\sigma} \sin(k_y a) \\ 2iu_{sp\sigma} \sin(k_x a) & E_{px}(\vec{k}) & -i\eta M_1 \\ 2iu_{sp\sigma} \sin(k_y a) & i\eta M_1 & E_{py}(\vec{k}) \end{pmatrix} \Psi_\eta, \quad (\text{A6})$$

$$H_{AB} = \sum_k \Psi_+^\dagger e^{i2k_x a_1} \begin{pmatrix} 2v_{s\sigma} \cos(k_z c/2) & -2v_{sp\sigma}\lambda_1 \cos(k_z c/2) & 0 \\ 2v_{sp\sigma}\lambda_1 \cos(k_z c/2) & 2 \cos(k_z c/2)(v_{p\pi}(1-\lambda_1^2) + v_{p\sigma}\lambda_1^2) & 0 \\ 0 & 0 & 2v_{p\pi} \cos(k_z c/2) \end{pmatrix} \Psi_- \quad (\text{A7})$$

where

$$\begin{aligned} E_s(\vec{k}) &= 2u_{s\sigma} [\cos(k_x a) + \cos(k_y a)] + \epsilon_s, \\ E_{px}(\vec{k}) &= 2[u_{p\sigma} \cos(k_x a) + u_{p\pi} \cos(k_y a)] + \epsilon_p, \\ E_{py}(\vec{k}) &= 2[u_{p\pi} \cos(k_x a) + u_{p\sigma} \cos(k_y a)] + \epsilon_p. \end{aligned} \quad (\text{A8})$$

Here $\Psi_\eta^\dagger = (c_{s\eta}^\dagger(\vec{k}), c_{p_x\eta}^\dagger(\vec{k}), c_{p_y\eta}^\dagger(\vec{k}))$, and $\vec{k} = \sum_{i=x,y,z} k_i \vec{e}_i$.

Next we would like to analyze the constraint on the form of Hamiltonian due to symmetry. In the main text, we have shown how the operations \hat{m}_z and \hat{g}_x act on the basis wave functions. The corresponding transformation matrices are given by

$$U(\hat{m}_z) = \begin{pmatrix} 1 & 0 \\ 0 & 1 \end{pmatrix}, \quad (\text{A9})$$

$$U(\hat{g}_x) = \begin{pmatrix} 0 & e^{-i(\hat{m}_x \vec{k}) \cdot \vec{\tau}} m_x \\ e^{-i(\hat{m}_x \vec{k}) \cdot \vec{\tau}} m_x & 0 \end{pmatrix}, \quad (\text{A10})$$

where

$$m_x = \begin{pmatrix} 1 & 0 & 0 \\ 0 & -1 & 0 \\ 0 & 0 & 1 \end{pmatrix} \quad (\text{A11})$$

and $\vec{\tau} = \frac{\vec{a}_3}{2} = (0, 0, \frac{c}{2})$.

$$H_\eta = \begin{pmatrix} E_s(\vec{k}) & \sqrt{2}iu_{sp\sigma} [\sin(k_x a) + i \sin(k_y a)] & -\sqrt{2}iu_{sp\sigma} [\sin(k_x a) - i \sin(k_y a)] \\ -\sqrt{2}iu_{sp\sigma} [\sin(k_x a) - i \sin(k_y a)] & \frac{1}{2}[E_{px}(\vec{k}) + E_{py}(\vec{k})] + \eta M_1 & -\frac{1}{2}[E_{px}(\vec{k}) - E_{py}(\vec{k})] \\ \sqrt{2}iu_{sp\sigma} [\sin(k_x a) + i \sin(k_y a)] & -\frac{1}{2}[E_{px}(\vec{k}) - E_{py}(\vec{k})] & \frac{1}{2}[E_{px}(\vec{k}) + E_{py}(\vec{k})] - \eta M_1 \end{pmatrix}. \quad (\text{A19})$$

From the Hamiltonian (A19), it is easy to see that the M_1 term serves as a Zeeman type of splitting for the states $|p_+\rangle$ and $|p_-\rangle$, which carry the angular momentum 1 and -1 , respectively. We may consider a simplified situation when

A symmetry of a Hamiltonian requires

$$H(\vec{k}) = U^*(\vec{k})H(\vec{U}\vec{k})U^T(\vec{k}). \quad (\text{A12})$$

In particular, the mirror symmetry \hat{m}_z yields

$$H_{A(B)}(k_x, k_y, k_z) = H_{A(B)}(k_x, k_y, -k_z), \quad (\text{A13})$$

$$H_{AB}(k_x, k_y, k_z) = H_{AB}(k_x, k_y, -k_z). \quad (\text{A14})$$

The glide symmetry results in

$$H_A(k_x, k_y, k_z) = m_x H_B(-k_x, k_y, k_z) m_x, \quad (\text{A15})$$

$$H_{AB}(k_x, k_y, k_z) = m_x H_{BA}(-k_x, k_y, k_z) m_x. \quad (\text{A16})$$

Moreover, since $|\alpha\eta, \vec{k} + \vec{G}\rangle = e^{i\vec{G}\cdot\vec{r}_0} |\alpha\eta, \vec{k}\rangle$, one find

$$H_{A(B)}(\vec{k} + \vec{G}) = H_{A(B)}(\vec{k}), \quad (\text{A17})$$

$$H_{AB}(\vec{k} + \vec{G}) = e^{i\vec{G}\cdot\vec{r}_0} H_{AB}(\vec{k}) \quad (\text{A18})$$

with $\vec{r}_0 = (2a_1, 0, \frac{c}{2})$. Equations (A13)–(A18) determine the form of our tight-binding Hamiltonian that respects the pmg symmetry group.

The coupling M_1 between magnetic moments and p orbitals plays an essential role in inducing topologically nontrivial phases, as shown in Ref. [26]. To see this, we may consider one layer with the effective Hamiltonian (A6) and change the basis from $|p_x\rangle$ and $|p_y\rangle$ to $|p_+\rangle = -\frac{1}{\sqrt{2}}(|p_x\rangle + i|p_y\rangle)$ and $|p_-\rangle = \frac{1}{\sqrt{2}}(|p_x\rangle - i|p_y\rangle)$. On the basis $|s\rangle$, $|p_+\rangle$, and $|p_-\rangle$, the effective Hamiltonian (A6) is rewritten as

the parameters of this model satisfy the condition $|E_s(\vec{k}) - E_p(\vec{k}) - M_1| \ll 2|M_1|$ where $E_p(\vec{k}) = \frac{1}{2}[E_{px}(\vec{k}) + E_{py}(\vec{k})]$. In this case, we can describe the low-energy physics with the $|s\rangle$ orbital and $|p_+\rangle$ ($|p_-\rangle$) orbital for the A (B) layer, given

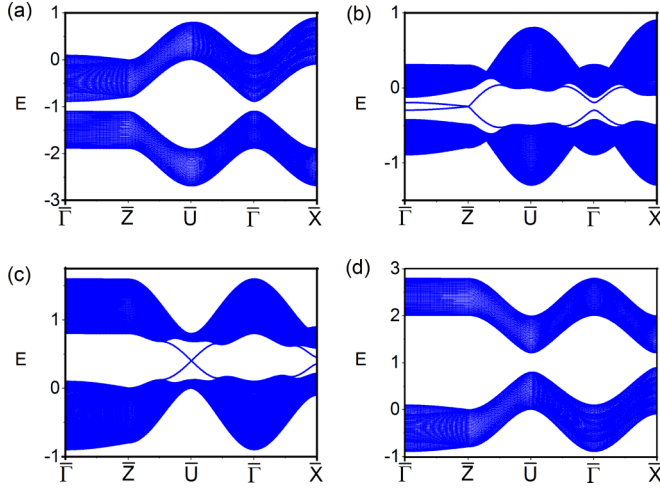


FIG. 4. (Color online) Energy dispersion of a slab configuration at different M_1 values: (a) $M_1 = 3.1 < 3.4$; the system is topologically trivial. (b) $3.4 < M_1 = 4.5 < 5$; the system is topologically nontrivial with a single gapless surface state at \bar{Z} . (c) $5 < M_1 = 5.8 < 6.6$; the system is topologically nontrivial with single gapless surface state at \bar{U} instead of \bar{Z} . (d) $M_1 = 7 > 6.6$; system is topologically trivial.

by a two-band effective Hamiltonian

$$H_{\text{eff},\eta} = \varepsilon(\vec{k}) + \sum_{i=x,y,z} d_i \sigma_i, \quad (\text{A20})$$

where σ is the Pauli matrix denoting the basis of s and p orbitals. For the A (B) layer ($\eta = \pm 1$), $\varepsilon(\vec{k}) = \frac{1}{2}[E_s(\vec{k}) + E_p(\vec{k}) + M_1]$, $d_x = -\sqrt{2}u_{sp\sigma} \sin(k_y a)$, $d_y =$

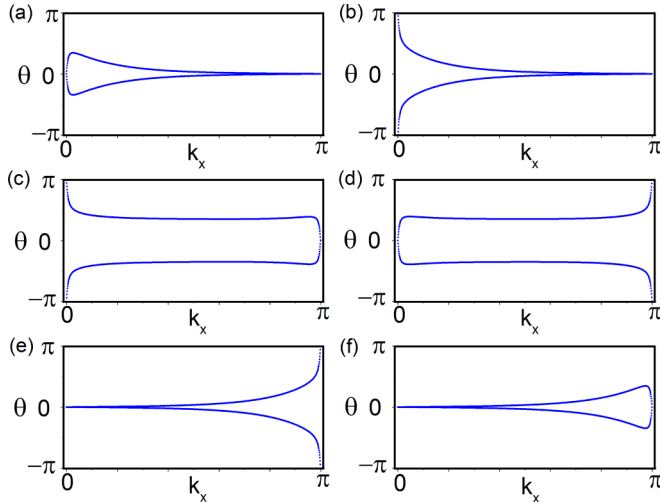


FIG. 5. (Color online) Wannier center flows for our tight-binding model characterizing three topological phase transitions (TPTs): First TPT at $M_1 = 3.4$: (a) $M_1 = 3.39$ (winding number = 0); (b) $M_1 = 3.41$ (winding number = 1). Second TPT at $M_1 = 5$ (this TPT shows no change in winding number because the band gap closes twice at the same time): (c) $M_1 = 4.99$ (winding number = 1); (d) $M_1 = 5.01$ (winding number = 1). Third TPT at $M_1 = 6.6$: (e) $M_1 = 6.59$ (winding number = 1); (f) $M_1 = 6.61$ (winding number = 0).

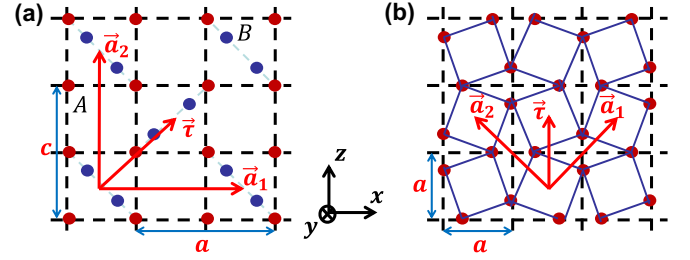


FIG. 6. (Color online) (a) A structure with pgg symmetry in the xz plane. Two lattice vectors are $\vec{a}_1 = (a, 0, 0)$ and $\vec{a}_2 = (0, 0, c)$, and the vector $\vec{\tau} = (\frac{a}{2}, 0, \frac{c}{2})$. A and B atoms are denoted by red and blue colors. Taking the point between two adjacent B atoms as the origin, two generators of the pgg group are $\{\hat{m}_x|\vec{\tau}\}$ and $\{\hat{m}_z|\vec{\tau}\}$. (b) A structure with $p4g$ symmetry in the xz plane. Two lattice vectors are $\vec{a}_1 = (a, 0, a)$ and $\vec{a}_2 = (-a, 0, a)$, and the vector $\vec{\tau} = (a, 0, 0)$. Two generators of the $p4g$ group are $\{C_4|\vec{\tau}\}$ and $\{\hat{m}_x|\vec{\tau}\}$.

$\mp\sqrt{2}u_{sp\sigma} \sin(k_x a)$, and $d_z = \frac{1}{2}[E_s(\vec{k}) - E_p(\vec{k}) - M_1]$. This model is known as the quantum anomalous Hall model, which has been well studied in Ref. [37]. It possesses a nonzero quantized Hall conductance when the configuration of the vector $\hat{d} = \frac{1}{d}(d_x, d_y, d_z)$ (where $d = \sqrt{\sum_i d_i^2}$) in the whole Brillouin zone has a nonzero winding number. By tuning the Zeeman splitting M_1 , the transition between trivial and nontrivial states can happen for each layer. This transition exactly corresponds to the transition between Z_2 trivial and nontrivial phases in our model after taking into account the coupling between A and B layers. In the following, we will numerically calculate the energy dispersion in a slab geometry with the open boundary condition along the y direction to test for the existence of gapless surface states. We choose the following set of parameters: $u_{s\sigma} = -0.2$, $u_{sp\sigma} = 0.2$, $u_{p\sigma} = 0.2$, $u_{p\pi} = 0.2$, $v_{s\sigma} = 0.05$, $v_{sp\sigma} = 0.3$, $v_{p\sigma} = -0.1$, $v_{p\pi} = 0.1$, $\epsilon_s = 0$, $\epsilon_p = -5$, $a = 1$, $a_1 = 0.1$, and $c = 2$. Combining both slab calculations and bulk dispersions, we find that band gaps close at three different M_1 values: (I) $M_1 = 3.4$; the system changes from being topologically trivial (no gapless surface state) to topologically nontrivial (single gapless surface state at \bar{Z}). (II) $M_1 = 5$; the system remains topologically nontrivial since the band gap closes at

TABLE I. The degeneracy of HSM in 2D nonsymmorphic groups for the single group case (spinless fermion or boson). Here ‘‘Factor group’’ is for the isomorphism class of the factor group of the 2D space group with respect to its translational subgroup and ‘‘Degeneracy’’ is for the degeneracy of electronic states at these momenta. ‘‘ Z_2 ’’ of the last column means whether Z_2 topological phases can exist in this nonsymmorphic group.

2D space group	HSM	Class	Factor group	Degeneracy	Z_2
pg	$\bar{\Gamma}, \bar{X}, \bar{Z}, \bar{U}$	K_0	D_1	1	no
	$\bar{\Gamma}, \bar{X}$	K_0	D_2	1	
pmg	\bar{Z}, \bar{U}	K_1	D_2	2	yes
	$\bar{\Gamma}, \bar{U}$	K_0	D_2	1	
pgg	\bar{X}, \bar{Z}	K_1	D_2	2	yes
	$\bar{\Gamma}, \bar{U}$	K_0	D_4	1 or 2	
$p4g$	\bar{X}, \bar{Z}	K_1	D_2	2	yes

TABLE II. The degeneracy of HSM in 2D nonsymmorphic groups for the double group case (spinful fermion).

2D space group	HSM	Class	Factor group	Degeneracy	Z_2
pg	$\bar{\Gamma}, \bar{X}, \bar{Z}, \bar{U}$	K_0	D_1	1	no
pmg	$\bar{\Gamma}, \bar{X}$	K_1	D_2	2	yes
	\bar{Z}, \bar{U}	K_0	D_2	1	
$p8g$	$\bar{\Gamma}, \bar{U}$	K_1	D_2	2	yes
	\bar{X}, \bar{Z}	K_0	D_2	1	
$p4g$	$\bar{\Gamma}, \bar{U}$	K_1	D_4	2	yes
	\bar{X}, \bar{Z}	K_0	D_2	1	

both T and U at the same time, similar to the case discussed in Ref. [8]. So the gapless surface states that appear at \bar{Z} previously moves to \bar{U} . (III) $M_1 = 6.6$; the system changes from being topologically nontrivial to topologically trivial.

Besides direct calculations of surface states, we can also extract the bulk topological invariant by tracking the evolution of Wannier function centers in the $k_z = \pi/c$ plane for our tight-binding model. For each fixed k_x , Wannier function centers can be obtained using a gauge-independent method introduced by Yu *et al.* [23]. For a one-dimensional system with periodic boundary conditions, the position operator is defined as

$$\hat{X} = \sum_{i,\alpha} e^{-i(2\pi/L)\cdot \mathbf{R}_i} |\alpha, i\rangle \langle \alpha, i|, \quad (\text{A21})$$

TABLE III. 3D space groups that can host surfaces with nonsymmorphic symmetries. In the brackets after the 3D space-group symbols, we list the number of the 3D space group and the Miller indices of the corresponding surfaces with nonsymmorphic symmetry groups.

Wallpaper group	3D space groups and the corresponding surfaces
	$Pma2(28, (001)), Aem2(39, (001)), Ama2(40, (001)), Imma2(46, (001)),$ $Pccm(49, (100), (010)), Pmma(51, (010)), Pmna(53, (010)), Pbcm(57, (100)),$ $Cmcm(63, (100)), Cmce(64, (010)), Cccm(66, (100), (010)), Cmme(67, (100), (010)),$ $Ibam(72, (100), (010)), Imma(74, (100), (010)), P4/mcc(124, (100), (010), (110), (1\bar{1}0)),$ $P4/nbm(125, (110), (1\bar{1}0)), P4/mnc(128, (110), (1\bar{1}0)), P4/nmm(129, (110), (1\bar{1}0)),$ $P4_2/mmc(131, (110), (1\bar{1}0)), P4_2/mcm(132, (100), (010)), P4_2/nmm(134, (110), (1\bar{1}0)),$ $P4_2/mbc(135, (110), (1\bar{1}0)), P4_2/nmc(138, (110), (1\bar{1}0)), I4/mcm(140, (100), (010)),$ $I4_1/amd(141, (100), (010)), P\bar{6}c2(188, (01\bar{1}0), (\bar{1}010), (1\bar{1}00)),$ $P\bar{6}2c(190, (\bar{1}2\bar{1}0), (\bar{1}\bar{1}20), (2\bar{1}\bar{1}0)),$ $P6/mcc(192, (01\bar{1}0), (\bar{1}010), (1\bar{1}00), (\bar{1}2\bar{1}0), (\bar{1}\bar{1}20), (2\bar{1}\bar{1}0)),$ $P6_3/mcm(193, (01\bar{1}0), (\bar{1}010), (1\bar{1}00)), P6_3/mmc(194, (\bar{1}2\bar{1}0), (\bar{1}\bar{1}20), (2\bar{1}\bar{1}0)),$ $Pm\bar{3}n(223, (110), (1\bar{1}0), (011), (01\bar{1}), (101), (\bar{1}01)),$ $Pn\bar{3}m(224, (110), (1\bar{1}0), (011), (01\bar{1}), (101), (\bar{1}01)),$ $Fm\bar{3}c(226, (110), (1\bar{1}0), (011), (01\bar{1}), (101), (\bar{1}01)),$ $Fd\bar{3}m(227, (110), (1\bar{1}0), (011), (01\bar{1}), (101), (\bar{1}01))$ $Pba2(32, (001)), Aea2(41, (001)), Iba2(45, (001)), Pban(50, (001)),$ $Pcca(54, (010)), Pbam(55, (001)), Cmce(64, (100)), Ccce(68, (100), (010)),$ $Ibam(72, (001)), Ibca(73, (001), (100), (010)), P4_2bc(106, (001)),$ $I4_1cd(110, (001)), P\bar{4}b2(117, (001)), I\bar{4}c2(120, (001)), P4/nnc(126, (110), (1\bar{1}0)),$ $P4/ncc(130, (110), (1\bar{1}0)), P4_2/nbc(133, (001), (110), (1\bar{1}0)), P4_2/mbc(135, (001)),$ $P4_2/nmc(137, (110), (1\bar{1}0)), I4_1/acd(142, (001), (100), (010)),$ $Ia\bar{3}(206, (001), (100), (010)), F\bar{4}3c(219, (001), (100), (010)),$ $Pn\bar{3}n(222, (110), (1\bar{1}0), (011), (01\bar{1}), (101), (\bar{1}01)),$ $Fd\bar{3}c(228, (001), (100), (010), (110), (1\bar{1}0), (011), (01\bar{1}), (101), (\bar{1}01)),$ $Ia\bar{3}d(230, (001), (100), (010))$ $I4cm(108, (001)), P4/nbm(125, (001)), P4/mbm(127, (001)),$ $I4/mcm(140, (001)), Fm\bar{3}c(226, (001), (100), (010))$
pmg	
$p8g$	
$p4g$	

where $L = N_y a$ is the length of the system, α is the orbital index, and i labels the lattice site. This position operator is defined using the local basis $|\alpha, i\rangle$, so its eigenvalues represent Wannier function centers of this system. By projecting this position operator into the occupied bands, it is easy to check that the projected position operator is equivalent to a $U(2N)$ Wilson loop for fixed k_x ,

$$D(k_x) = S_{0,1} S_{1,2} S_{2,3} \dots S_{N_y-2, N_y-1} S_{N_y-1, 0}, \quad (\text{A22})$$

where a series of overlap matrices S are defined using the periodic parts of Bloch wave functions,

$$S_{i,i+1}^{m,n}(k_x) = \langle m, k_{y,i}, k_x | n, k_{y,i+1}, k_x \rangle$$

$$k_{y,i} = \frac{2\pi i}{N_y a}. \quad (\text{A23})$$

Then the phases of the eigenvalues of this $U(2N)$ Wilson loop $D(k_x)$ just give us Wannier centers of the occupied bands. By letting k_x evolve from 0 to π/a , we could clearly see whether the Wannier centers switch partners (when the winding number is odd and the system is topologically nontrivial) or not (when the winding number is even and the system is topologically trivial). As is shown in both Figs. 4 and 5, the winding numbers of Wannier function centers precisely characterize topological phase transitions and the appearance of surface states.

APPENDIX B: SPACE-GROUP TABLES FOR TOPOLOGICAL NONSYMMORPHIC CRYSTALLINE INSULATORS

Figures 6(a) and 6(b) show the example structures for pgg and $p4g$ symmetry group, respectively. Here we take the surface normal be to the y direction and assume the lattice along the y direction preserves the 2D symmetry group of the surface. Thus, the degeneracies found in the surface BZ are preserved along the whole k_y line in the 3D bulk BZ, which allows us to define a Z_2 topological invariant in a way similar to the case of pmg .

The Tables I and II give the possible 2D space groups for the surfaces that can host topological nonsymmorphic crystalline insulators in the spinless and spinful systems, respectively. The essential step is to determine the degeneracy of HSM for the corresponding symmetry group based on the projective representation theory [22]. We have shown how to determine the factor system and the corresponding projective representation for the single group case, which is applicable to spinless fermions and bosons. The generalization to the double group (spinful fermions) is quite straightforward. In this case, at a momentum \vec{k} the representation matrix takes the form $D_{\vec{k}}(\{S|\vec{R}\}) = e^{i\vec{k}\cdot\vec{R}}\mathcal{D}(S)\chi(S)$ for the symmetry operator $\{S|\vec{R}\}$, where $\mathcal{D}(S)$ is for the spatial part and $\chi(S)$ is for the spin part. Now the factor system is determined by the phase factor $\omega(S_1, S_2)$ defined as $\mathcal{D}(S_1)\mathcal{D}(S_2) = \omega(S_1, S_2)\mathcal{D}(S_1S_2)$ for two operators $\{S_1|\vec{R}_1\}$ and $\{S_2|\vec{R}_2\}$. Therefore, it is easy to see that the spin part $\chi(S)$ gives an additional contribution to the phase factor $\omega(S_1, S_2)$. To determine to which class

the projective representation belongs, one needs to consider the parameter $\alpha = \frac{\omega(S_1, S_2)}{\omega(S_2, S_1)}$. Therefore, it is essential how two operators S_1 and S_2 act on the spin part. Let us consider the example of pmg group. For the operators \hat{m}_z and $\hat{g}_x = \{\hat{m}_x|\vec{\tau}\}$, since $\chi(\hat{m}_z) = i\sigma_z$ anticommutes with $\chi(\hat{m}_x) = i\sigma_x$ (σ_x and σ_z are two Pauli matrices), one can show that $\alpha = -1$ for $\vec{K} = \vec{\Gamma}, \vec{X}$ and $\alpha = 1$ for $\vec{K} = \vec{Z}, \vec{U}$ for the spinful case, which is exactly opposite to the spinless case. The results for other 2D nonsymmorphic space groups are summarized in Table II.

Table III gives the corresponding 3D space groups that can have surfaces with the required 2D space-group symmetry.

To identify the symmetry groups on specific surfaces, we make use of the concept of layer groups. By comparing their symmetry operations, we arrive at the following correspondence between 2D space groups and layer groups:

$$pmg \text{ group} \Rightarrow \text{Layer group 24,}$$

$$pgg \text{ group} \Rightarrow \text{Layer group 25,}$$

$$p4g \text{ group} \Rightarrow \text{Layer group 56.}$$

This correspondence is such that the layer group is isomorphic to the space group. Then Table III can be obtained with the help of the scanning tables found in Volume E of the International Tables for Crystallography, Ref. [38].

Finally, based on Table III, one can easily identify appropriate systems to look for. For example, the surfaces with pmg symmetry group can exist in many compounds of iron pnictides and chalcogenides ($P4/nmm$ group) [39–42] and some antiferromagnetic materials with the spinel structures ($Fd\bar{3}m$) [43,44].

-
- [1] X. L. Qi and S. C. Zhang, *Phys. Today* **63**(1), 33 (2010).
 [2] M. Z. Hasan and C. L. Kane, *Rev. Mod. Phys.* **82**, 3045 (2010).
 [3] J. E. Moore, *Nature (London)* **464**, 194 (2010).
 [4] X.-L. Qi and S.-C. Zhang, *Rev. Mod. Phys.* **83**, 1057 (2011).
 [5] C. L. Kane and E. J. Mele, *Phys. Rev. Lett.* **95**, 146802 (2005).
 [6] L. Fu, *Phys. Rev. Lett.* **106**, 106802 (2011).
 [7] T. H. Hsieh, H. Lin, J. Liu, W. Duan, A. Bansil, and L. Fu, *Nat. Commun.* **3**, 982 (2012).
 [8] R.-J. Slager, A. Mesaros, V. Juričić, and J. Zaanen, *Nat. Phys.* **9**, 98 (2012).
 [9] C. Fang, M. J. Gilbert, and B. A. Bernevig, *Phys. Rev. B* **86**, 115112 (2012).
 [10] P. Jadaun, D. Xiao, Q. Niu, and S. K. Banerjee, *Phys. Rev. B* **88**, 085110 (2013).
 [11] C. Fang, M. J. Gilbert, X. Dai, and B. A. Bernevig, *Phys. Rev. Lett.* **108**, 266802 (2012).
 [12] M. Kargarian and G. A. Fiete, *Phys. Rev. Lett.* **110**, 156403 (2013).
 [13] Y. Ueno, A. Yamakage, Y. Tanaka, and M. Sato, *Phys. Rev. Lett.* **111**, 087002 (2013).
 [14] Y. Tanaka, T. Sato, K. Nakayama, S. Souma, T. Takahashi, Z. Ren, M. Novak, K. Segawa, and Y. Ando, *Phys. Rev. B* **87**, 155105 (2013).
 [15] J. Liu, W. Duan, and L. Fu, *Phys. Rev. B* **88**, 241303 (2013).
 [16] C. Fang, M. J. Gilbert, S.-Y. Xu, B. A. Bernevig, and M. Z. Hasan, *Phys. Rev. B* **88**, 125141 (2013).
 [17] I. Fulga, B. van Heck, J. Edge, and A. Akhmerov, *Phys. Rev. B* **89**, 155424 (2014).
 [18] P. Dziawa, B. Kowalski, K. Dybko, R. Buczko, A. Szczerbakow, M. Sztot, E. Łusakowska, T. Balasubramanian, B. M. Wojek, M. Berntsen, O. Tjernberg, and T. Story, *Nat. Mater.* **11**, 1023 (2012).
 [19] Y. Tanaka, Z. Ren, T. Sato, K. Nakayama, S. Souma, T. Takahashi, K. Segawa, and Y. Ando, *Nat. Phys.* **8**, 800 (2012).
 [20] S.-Y. Xu, C. Liu, N. Alidoust, M. Neupane, D. Qian, I. Belopolski, J. Denlinger, Y. Wang, H. Lin, L. Wray, G. Landolt, B. Slomski, J. Dil, A. Marcinkova, E. Morosan, Q. Gibson, R. Sankar, F. Chou, R. Cava, A. Bansil, and M. Hasan, *Nat. Commun.* **3**, 1192 (2012).
 [21] M. S. Dresselhaus, G. Dresselhaus, and A. Jorio, *Group Theory: Application to the Physics of Condensed Matter* (Springer-Verlag, Berlin, Heidelberg, 2008).
 [22] G. L. Bir and G. E. Pikus, *Symmetry and Strain-induced Effects in Semiconductors* (House Jerusalem Ltd., Jerusalem, London, 1974).
 [23] R. Yu, X. L. Qi, A. Bernevig, Z. Fang, and X. Dai, *Phys. Rev. B* **84**, 075119 (2011).
 [24] R. S. K. Mong, A. M. Essin, and J. E. Moore, *Phys. Rev. B* **81**, 245209 (2010).

- [25] C. Fang, M. J. Gilbert, and B. A. Bernevig, *Phys. Rev. B* **88**, 085406 (2013).
- [26] C.-X. Liu, [arXiv:1304.6455](https://arxiv.org/abs/1304.6455) (2013).
- [27] See Supplemental Material at <http://link.aps.org/supplemental/10.1103/PhysRevB.90.085304> for our tight-binding model, the calculation of surface states, and Z_2 topological invariants and the table for possible topological phases in different nonsymmorphic space groups.
- [28] L. Fu and C. L. Kane, *Phys. Rev. B* **76**, 045302 (2007).
- [29] A. Alexandradinata, C. Fang, M. J. Gilbert, and B. A. Bernevig, [arXiv:1402.6323](https://arxiv.org/abs/1402.6323) (2014).
- [30] C.-Z. Chang, J. Zhang, X. Feng, J. Shen, Z. Zhang, M. Guo, K. Li, Y. Ou, P. Wei, L.-L. Wang, Z.-Q. Ji, Y. Feng, S. Ji, X. Chen, J. Jia, X. Dai, Z. Fang, S.-C. Zhang, K. He, Y. Wang, L. Lu, X.-C. Ma, and Q.-K. Xue, *Science* **340**, 167 (2013).
- [31] V. Yannopapas, *Phys. Rev. B* **84**, 195126 (2011).
- [32] Z. Wang, Y. Chong, J. D. Joannopoulos, and M. Soljačić, *Nature (London)* **461**, 772 (2009).
- [33] M. C. Rechtsman, J. M. Zeuner, Y. Plotnik, Y. Lumer, D. Podolsky, F. Dreisow, S. Nolte, M. Segev, and A. Szameit, *Nature (London)* **496**, 196 (2013).
- [34] R. Roy, [arXiv:1212.2944](https://arxiv.org/abs/1212.2944) (2012).
- [35] S. A. Parameswaran, A. M. Turner, D. P. Arovas, and A. Vishwanath, *Nat. Phys.* **9**, 299 (2013).
- [36] X. Chen, Z.-C. Gu, Z.-X. Liu, and X.-G. Wen, *Science* **338**, 1604 (2012).
- [37] X. L. Qi, Y. S. Wu, and S. C. Zhang, *Phys. Rev. B* **74**, 085308 (2006).
- [38] V. Kopsky and D. B. Litvin, *Subperiodic Groups*, International Tables for Crystallography Vol. E, 1st online ed. (International Union of Crystallography, Dordrecht, The Netherlands, 2006).
- [39] Y. Kamihara, T. Watanabe, M. Hirano, and H. Hosono, *J. Am. Chem. Soc.* **130**, 3296 (2008).
- [40] J. Hu, *Phys. Rev. X* **3**, 031004 (2013).
- [41] F. Ma, W. Ji, J. Hu, Z.-Y. Lu, and T. Xiang, *Phys. Rev. Lett.* **102**, 177003 (2009).
- [42] C. de La Cruz, Q. Huang, J. Lynn, J. Li, W. Ratcliff II, J. L. Zarestky, H. Mook, G. Chen, J. Luo, N. Wang *et al.*, *Nature (London)* **453**, 899 (2008).
- [43] V. Brabers and A. Broemme, *J. Magn. Magn. Mater.* **104**, 405 (1992).
- [44] W. Roth, *J. Phys. Chem. Solids* **25**, 1 (1964).